

## HOVERING FLIGHT IN THE PIED FLYCATCHER (FICEDULA HYPOLEUCA)

U. M. Norberg

University of Göteborg

Göteborg, Sweden

### ABSTRACT

Slow-motion films (200 frames/sec) taken in the field on a freely hovering pied flycatcher, Ficedula hypoleuca (Pallas), are used for description of the kinematics and for calculation of an average coefficient of lift,  $\bar{C}_L$ , in hovering flight. Using Weis-Fogh's (1972) equations for steady-state aerodynamics, and assuming that the upstroke gives no useful forces, the average lift coefficient is estimated to be about 5.3. Since this high value of  $\bar{C}_L$  is not consistent with steady-state aerodynamics, non-steady-state phenomena must be of large importance.

### INTRODUCTION

Hovering flight is performed by most insects and by many small birds and bats. Hummingbirds and insects hover with fully extended wings during the entire wing-stroke cycle, and hence useful forces can be elicited during most parts of the cycle. Normal hovering is defined by Weis-Fogh (1973) as active flight on the spot with wings moving through a large stroke angle and approximately in a horizontal plane while the long axis of the body is strongly inclined to the horizontal. Hovering flight in several small passerine birds (Zimmer (1943), Brown (1951), Greenewalt (1960)) and bats (Norberg (1970)) differ somewhat from normal hovering.

Weis-Fogh showed that hovering flight in hummingbirds and Drosophila (1972) is consistent with steady-state aerodynamics, and later (1973) he showed that hovering flight in several insects

can be explained by steady-state aerodynamics. The purpose of the present investigation is to find out if hovering flight in the pied flycatcher, Ficedula hypoleuca (Pallas), can be understood on the basis of steady-state aerodynamics or if it has to be explained by non-steady-state phenomena.

A description of the kinematics is given, and film data are used for calculation of an average minimum coefficient of lift.

## MATERIAL AND METHODS

Slow-motion films (200 frame  $\text{sec}^{-1}$ ) were taken with a Mitchell 16 mm high-speed film camera on a hovering pied flycatcher in the field. Filming was performed at a nest-box in calm weather. A leaf was put in the entrance of the nest-box, which caused the flycatcher to hesitate and hover in front of it for several seconds before alighting to feed insects to the young. Lateral and posterior views were obtained. No artificial light was used in filming. Still pictures were taken with a Leicaflex SL camera with the aid of electronic flash (flash duration 0.1 msec). Films used were 16 mm Kodak Ektachrome EF and 35 mm Kodak Panatomic-X, respectively.

Data on weight, wing length and wing area were obtained from specimens other than the one filmed. The weight has been measured by Hansson et al. (1965;  $W = 125 \text{ N}$ ,  $n = 75$ ) and by Silverin (personal communication;  $W = 117 \text{ N}$ ,  $n = 40$ ) during the period when the birds were feeding young.

The bird is assumed to make use of steady-state aerodynamics, and the aim is to calculate the average lift coefficient  $\overline{C}_L$ , which can be regarded as the minimum coefficient of lift which must be ascribed to the wings. This value of  $\overline{C}_L$  must not exceed the maximum coefficient of lift obtainable at the Reynolds number under which the wings operate, if steady-state aerodynamics are adequate to explain hovering flight (Weig-Fogh (1972)). The average lift coefficient  $\overline{C}_L$  is estimated by using the equations of Weis-Fogh (1972).

## CALCULATION OF THE COEFFICIENT OF LIFT

The resulting aerodynamic force is vertical and equal to the body weight when averaged over a whole wing-stroke. The upstroke is assumed to give no useful forces (see below), and thus the vertical forces elicited during the downstroke must be larger than the body weight. In all the calculations the movements normal to the stroke plane are disregarded.

Data are taken from a single stroke (no. 5 in Figure 1 judged to be representative) where the downstroke lasts ca. 30 msec and the upstroke ca. 40 msec. The wing movements (angular movement of the long wing-axis) during the downstroke is almost sinusoidal (Figure 1).

Using the equations of Weis-Fogh (1972) the resulting aerodynamic force (Figure 7) is

$$F_r = 1/2 \rho V_r^2 A_r C_L / \cos \chi, \quad (1)$$

where  $\rho$  is air density,  $V_r$  is relative wind (the resultant of flapping velocity  $v_r$  and induced wind  $w$ ),  $A_r$  is area of a strip at distance  $r$  from the fulcrum, and  $\tan \chi$  equals  $C_D/C_L$ . The vertical component  $H_r$  of  $F_r$  is

$$H_r = 1/2 \rho V_r^2 A_r C_L \cos(\chi + \psi) / \cos \chi. \quad (2)$$

Angle  $\psi$  equals  $\delta - \beta$ , where  $\beta$  is the angle of tilt of the stroke path, and  $\sin \delta = w \cos \beta / V_r$ .

A lift:drag ratio ( $L/D$ ) of 5 is used. Ratios of about this size were estimated by Pennycuik (1969) for small passerine birds. The wing was divided into ten strips (1-10, Figure 8), each 1 cm wide, and their areas were measured. The radius  $r$  was measured from the fulcrum to the middle of each strip,  $r_1$  being 0.5 cm,  $r_2$  1.5 cm, etc.  $H_r/C_L$  was calculated from equation (2) for each of the ten strips for seven time-equidistant points during a half downstroke. The average value of  $H_r/C_L$  can be found by integrating the summed curves for all strips of both wings with respect to the time for a whole downstroke, and then dividing by the time for a whole wingstroke. The vertical force,  $H_r$ , as averaged over a whole wingstroke, must equal the weight  $\bar{W}$  of the bird, and hence the minimum average value of  $C_L$  can be found. Integration was performed graphically.

## RESULTS

### Flight Parameters and Kinematics

The basic flight data used are listed in Table I. Seven representative wing-strokes were analysed. These were preceded by several hovering strokes. The wing tip path is almost ellipsoidal and the inclination of the stroke path is ca.  $30^\circ$  to the horizontal (Figure 2). The long axis of the body is inclined  $40-50^\circ$

TABLE I  
BASIC PARAMETERS FOR HOVERING FLIGHT IN  
FICEDULA HYPOLEUCA

Body weight, $W$	0.1177 N
Wing-length	0.10 m
Wing-span	0.23 m
Wing-area (one wing), $A$	$0.00451 \text{ m}^2$
Wing-loading	$13.05 \text{ Nm}^{-2}$
Stroke angle, $\phi$	$102^\circ = 1.78 \text{ rad}$
Stroke frequency, $n$	$14.3 \text{ sec}^{-1}$
Duration of downstroke	30 msec
which would correspond to a stroke frequency of $16.7 \text{ sec}^{-1}$ if upstroke were of equal length	
Duration of upstroke	40 msec
Angle of tilt of wing tip path, $\beta$	$30^\circ$
Induced wind, $w$	$1.08 \text{ msec}^{-1}$
Adopted $C_L/C_D$	5
Air density, $\rho$	$1.22 \text{ kgm}^{-3}$

to the horizontal. The duration of each of the seven wing-strokes studied varied between 50 and 90 msec corresponding to 20 and 11.8 strokes  $\text{sec}^{-1}$  (Figure 1). The bird often slows down the movement of the wings for a short moment during the upstroke (strokes 3, 4, and 7 in Figure 1), just as it often does during forward flight, hence this large variation of the stroke frequency. The downstroke lasts 25-30 msec, the upstroke 25-60 msec (Figure 1). The movement of the long wing axis is almost sinusoidal with respect to angular displacement. The stroke angle is defined as the angle formed between straight lines from the shoulder joint to the wing tip at its reversal points. It is ca.  $102^\circ$ .

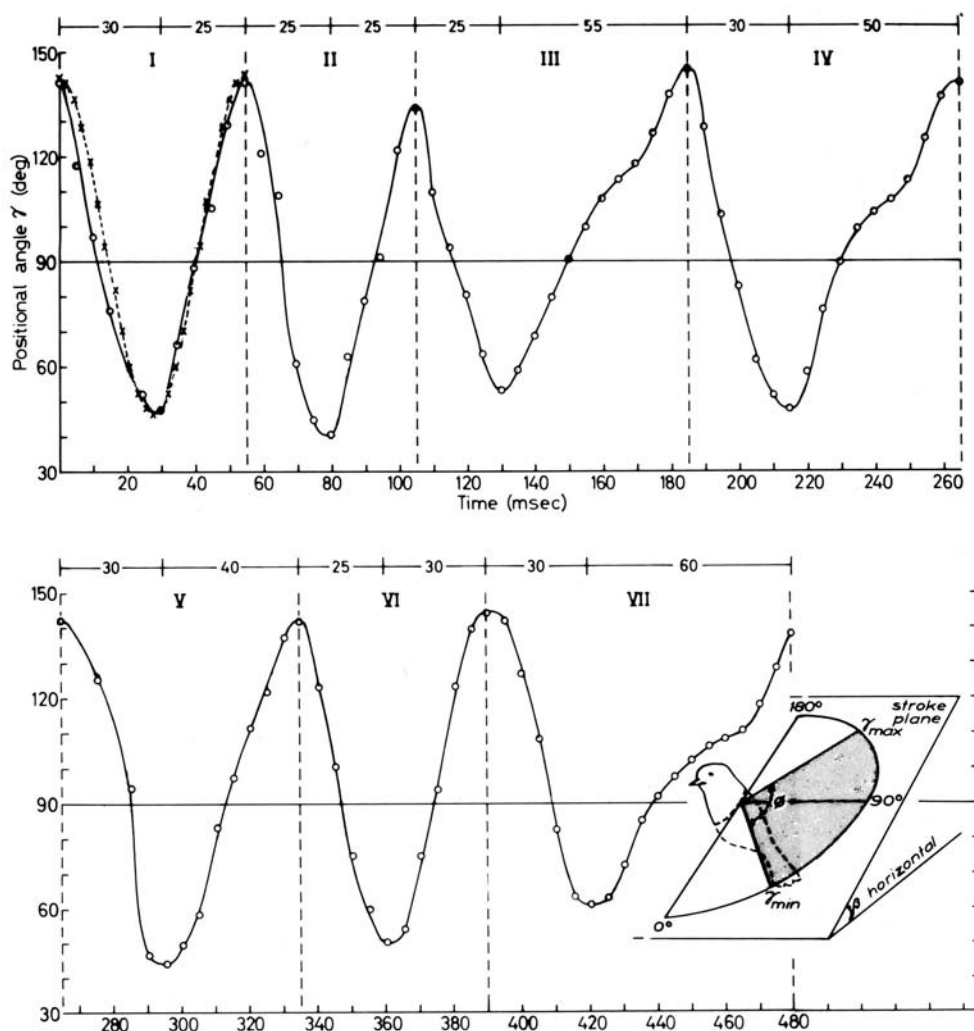


Figure 1. The angular movements of the long axis of the wing relative to the body during seven wing-strokes in hovering flight of *Ficedula hypoleuca*. During the upstrokes in stroke numbers 3, 4, and 7, the movements are slowed down. The exposure rate was 200 frames per sec. The broken curve shows a sinusoidal movement for comparison.

During the downstroke the wings are fully extended, cambered and multislotted in their outer parts, i.e. the alula is raised and the free ends of the hand remiges are separated, letting air through (Figures 3 and 4). At the beginning of the downstroke the wings are slightly pronated. The tip feathers are bent upwards,

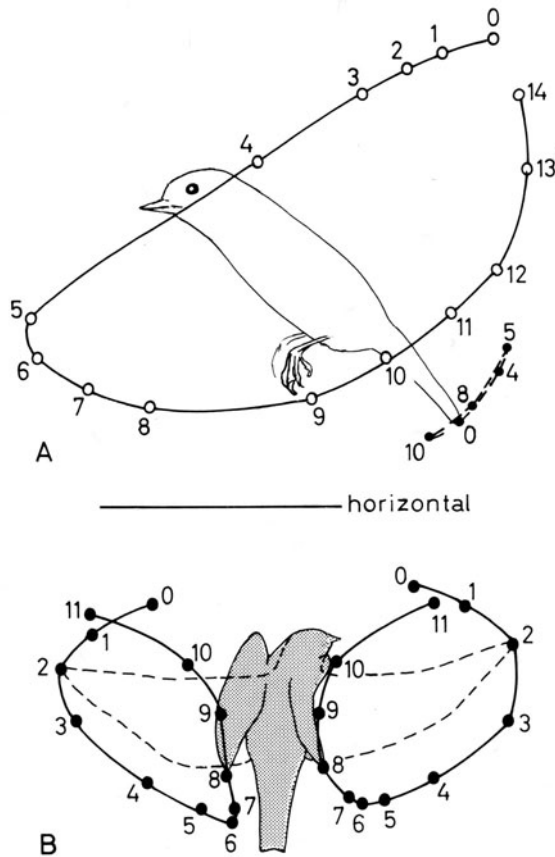
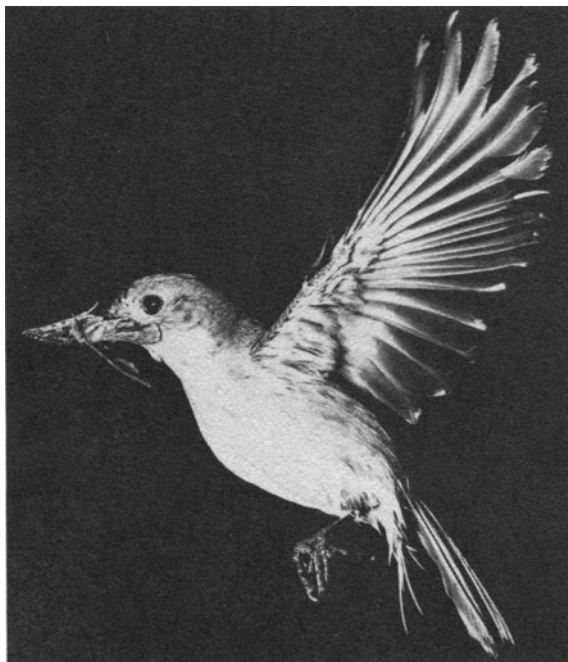


Figure 2. Tracks of the wing-tips and tail of *Ficedula hypoleuca* in hovering flight. A. Lateral view (left wing). B. Posterior view (note the strong flexing of the wings during the upstroke). The numbers indicate each 200th of a second from the uppermost position of the wings.

indicating a vertical resultant force (Figures 3 and 4). At the middle of the downstroke the speed of the wing-tip is ca.  $8.8 \text{ msec}^{-1}$ .

At the beginning of the upstroke the wings are strongly flexed at the elbow and wrist (Figure 5). They are elevated near to the body, and the primaries are rotated in the nose-up sense close to a feathered position. The hand wing therefore becomes split by deep slits (extending nearly to the wrist) letting air through (Figures 5 and 6). During the upstroke the movement of the long wing-axis sometimes is sinusoidal with respect to angular displacement, and sometimes it is not, due to a slow down of the wing movement during the upstroke (Figure 1). At the end of the



(Figures 3-6 Ficedula hypoleuca in hovering flight.)

Figure 3. Position of wings in the beginning of the downstroke.  
Photo Ulla M. Norberg.



Figure 4. Position of the wings in the later part of the downstroke.  
Photo Ulla M. Norberg.

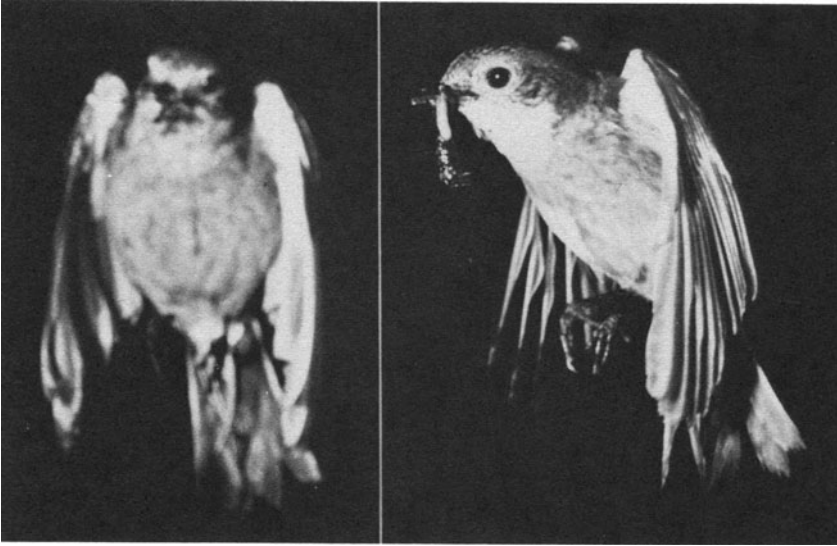


Figure 5. Position of wings in the beginning of the upstroke. The wings are strongly flexed. The primaries are rotated in the nose-up sense, letting air through. Photo Ulla M. Norberg



Figure 6. Position of wings in the later part of the upstroke. They are gradually extended again. Photo R. Åke Norberg.



upstroke the bases of the arm wings meet at their rear parts, i. e. the tips of the left and right secondaries meet, before the wings are fully extended again.

The tail is moved up during the downstroke and down during the upstroke (Figure 2). These movements seem to be performed to prevent the body from rotating alternately in a nose-down and nose-up sense due to changing rotating moments caused by aerodynamic and inertial forces of the wings.

### Coefficient of Lift

Figure 8 shows the variation of  $H_r/C_L$  with relative time. At  $t_0 = 0$  msec the wing passes the middle position ( $\gamma = 90^\circ$ ) and at  $t_6 = 15$  msec, the wing is at one extreme position. The weight

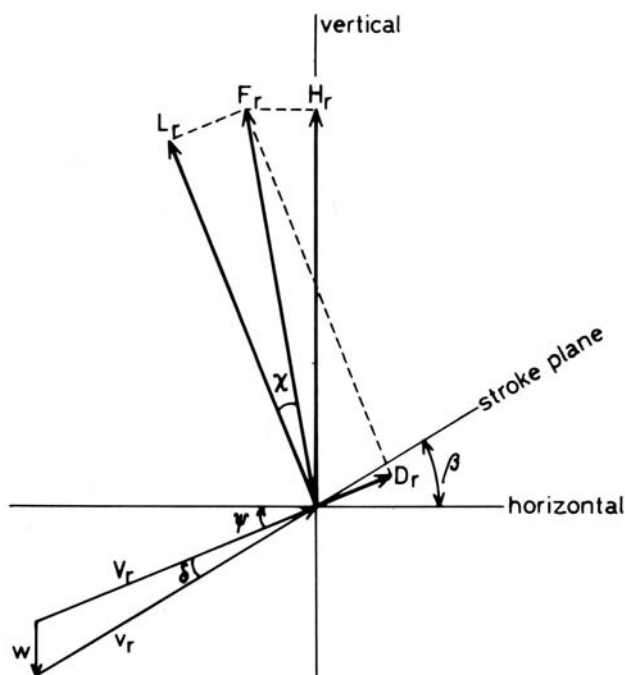


Figure 7. The velocity and force systems acting on a wing-element at a distance  $r$  from the fulcrum during hovering flight. The figure is based on data at strip no. 7 at the middle of the downstroke.  $v_r$  is the flapping velocity,  $w$  the induced wind,  $V_r$  the relative velocity, and  $\beta$  the angle of tilt of the stroke plane relative to the horizontal. The  $L/D$  ratio is 5.  $H_r$  is the vertical component of the resulting force  $F_r$ .

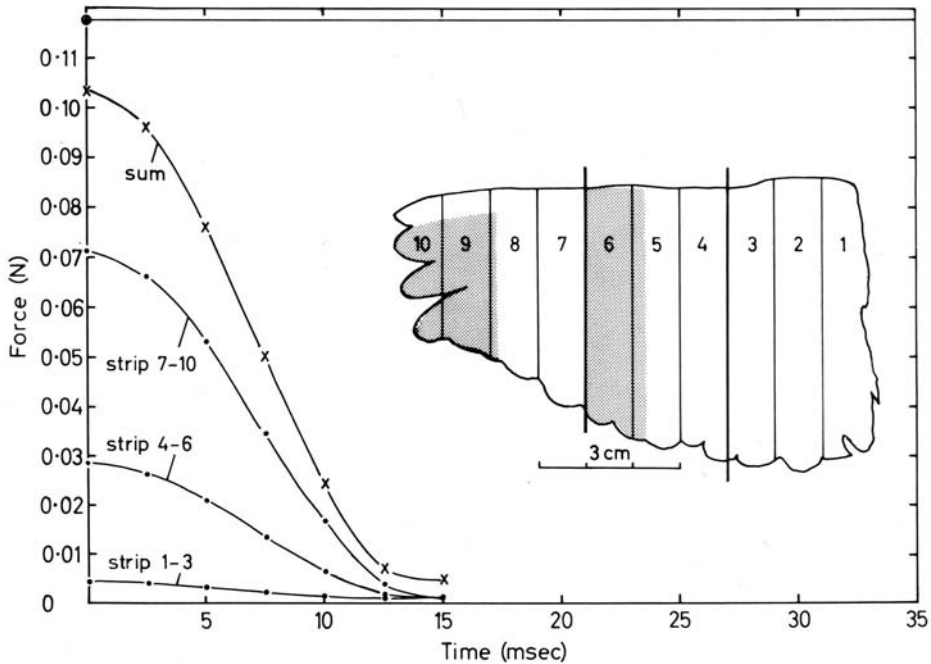


Figure 8. The ten wing-strips in *Ficedula hypoleuca*, and the values of  $H_r/C_L$  for each section, 1-10, as it varies with the relative time,  $t$ , during half a downstroke in hovering flight. The weight of the bird is indicated by an open circle on the ordinate axis. The area under the summed curve must be multiplied by such a value of  $C_L$  (here 5.3) as to make the product equal to the area under the straight line during the time for half a downstroke and half an upstroke.

of the bird is indicated on the ordinate axis. A horizontal straight line has been drawn from it to  $t = 35$  msec, which is half the time of a complete stroke cycle. Since the upstroke is assumed to give no useful forces, the downstroke must give all the vertical forces which are to balance the weight of the bird during the complete stroke cycle. Therefore the area under the summed curve in Figure 8, which gives the value of  $H_r/C_L$  for both wings as integrated over half a downstroke, must be multiplied by a value of  $C_L$ , so chosen as to make the integral of  $H_r$  equal to the area under the horizontal straight line which covers half a downstroke plus half an upstroke. The average lift coefficient for *Ficedula* is estimated to be ca. 5.3. As can be seen from Figure 8 the inner third (strips 1-3) of the wing has little aerodynamic effect, only about 4.1%.

## DISCUSSION

Unlike the hummingbird, the pied flycatcher is not so well anatomically adapted for hovering flight. The pied flycatcher's hand wing is relatively shorter and it is not able to perform the rotating movement at the shoulder joint, which makes it possible for hummingbirds to turn the upside of the wing down during the morphological upstroke. Hovering is a common habit in hummingbirds, while the pied flycatcher hovers only for short periods when snapping insects in the air. The latter usually searches for and detects insects from a perch and then makes short flights to catch them. It is in connection with the actual catching that hovering flight is most often used.

In the pied flycatcher the upstroke in hovering seems to be very inefficient and can hardly contribute any vertical upward force, at least not when only steady-state aerodynamics are considered. Therefore the average coefficient of lift must be very high, and is calculated to be about 5.3. This means that hovering flight in this bird is not consistent with steady-state aerodynamics, and must be explained to a large part by non-steady-state principles. If the upstroke would be as effective as the downstroke, the value of  $C_L$  would be half of that estimated. Also that would be very high for steady-state aerodynamics, but may be possible because of the multislot wing. Slots prevent flow separation at the upper surface of the wing area behind the slots. Therefore larger angles of attack may be used without stalling, and hence larger lift coefficients can be achieved. Nachtigall and Kempf (1971) made wind-tunnel measurements on wings of Passer domesticus, Turdus merula, and Anas platyrhynchos, and found lift enhancing effects of the alula of up to 25% during steady-state conditions. During the downstroke the slotted areas posterior to the alula and the free hand remiges make up ca. 24% of the wing area in Ficedula hypoleuca (Figure 8). When the effect of the slots is not considered, ca. 37% of the aerodynamic force of the wing comes from the slotted parts. The slots tend to increase the force contribution from these areas, while pressure equalization around the tip tends to decrease it. The net effect of this is not known.

When the wing is in the middle of the downstroke, i. e. at  $V_{max}$ , the Reynolds number at  $0.7 r$  is ca. 17300. The distance travelled by the wing chord at  $0.7 r$  during half a stroke is only ca. 3.3 chord lengths. It takes 2-3 chord lengths before steady-state lift is built up after the reversal points - the Wagner effect (cf. Weis-Fogh (1972) p. 97). This tends to make the beginning of a stroke less efficient. However, this effect is counteracted by delayed stall, which permits large angles of attack and hence

large aerodynamic forces at the beginning of a stroke. What the net outcome of this will be is not known. This needs further study.

At the upper reversal point the bases of the arm wings meet at their rear parts, i. e. the tips of the left and right proximal secondaries meet. This clapping together of the trailing edges of the arm wings and subsequent separation of the arm wings might create lift according to the "flight mechanism", described by Weis-Fogh (1973) and Lighthill (1973). This is a mechanism for setting up circulation over the wing and thus creating lift. However, since only the arm wings of the flycatcher are involved, this mechanism if it occurs here, probably is of little importance. The hand wings are angled outwards and do not meet at the upper reversal point of the wingstroke.

#### ACKNOWLEDGMENTS

I am indebted to Civ. ing. Tryggve Ramquist, FOA, Stockholm, for taking the high speed film, and to Fil. mag. Bengt Silverin, Department of Zoology, Göteborg, for letting me use his unpublished data on weight of the pied flycatcher.

#### REFERENCES

- Brown, R. H. J. 1951 Flapping flight. *Ibis*, 93, 333-359.
- Greenewalt, C. H. 1960 Hummingbirds. Doubleday, New York.
- Hansson, S. Å., Lennerstedt, I., Myhrberg, H., and Nyholm, E. 1966 Holstudier vid Ammarnäs 1965. *Fauna och Flora*, 6, 225-254. In Swedish, English summary (Nest box studies at Ammarnäs in 1965)
- Lighthill, M. J. 1973 On the Weis-Fogh mechanism of lift generation. *J. fluid Mech.* 60, 1-17.
- Nachtigall, W. and Kempf, B. 1971 Vergleichende Untersuchungen zur flugbiologischen Funktion des Daumenfittichs (*Alula spuria*) bei Vögeln. *Z. vergl. Physiol.* 71, 326-341.
- Norberg, U. M. 1970 Hovering flight of Plecotus auritus Linnaeus. *Proc. 2nd Int. Bat Res. Conf.*, 62-66.
- Pennycuik, C. J. 1969 The mechanics of bird migration. *Ibis*, 111, 525-556.
- Weis-Fogh, T. 1972 Energetics of hovering flight in hummingbirds and in *Drosophila*. *J. Exp. Biol.* 56, 79-104.

Weis-Fogh, T. 1973 Quick estimates of flight fitness in hovering animals, including novel mechanisms for lift production. J. Exp. Biol. 59, 169-230.

Zimmer, K. 1943 Der Flug des Nektarvogels (Cinnyris). J. Orn. Lpz. 91, 371-387.